ac susceptibility investigation of vortex dynamics in nearly optimally doped RFeAsO1−xFx superconductors (R = La, Ce, Sm)

ac susceptibility investigation of vortex dynamics in nearly optimally doped $R\mathrm{FeAsO}_{1-x}\mathrm{F}_x$ superconductors (R = La, Ce, Sm)

G. Prando,[1,2,*] P. Carretta,[1] R. De Renzi,[3] S. Sanna,[1] H.-J. Grafe,[4] S. Wurmehl,[4] and B. Büchner[4]

[1]*Department of Physics "A. Volta," University of Pavia-CNISM, I-27100 Pavia, Italy*

[2]*Department of Physics "E. Amaldi," University of Roma Tre-CNISM, I-00146 Roma, Italy*

[3]*Department of Physics, University of Parma-CNISM, I-43124 Parma, Italy*

[4]*Leibniz-Institut für Festkörper- und Werkstoffforschung (IFW) Dresden, D-01171 Dresden, Germany*

(Received 17 December 2011; revised manuscript received 17 February 2012; published 24 April 2012)

Ac susceptibility and static magnetization measurements were performed in the nearly optimally doped $\mathrm{LaFeAsO}_{0.9}\mathrm{F}_{0.1}$ and $\mathrm{CeFeAsO}_{0.92}\mathrm{F}_{0.08}$ superconductors, complementing earlier results on $\mathrm{SmFeAsO}_{0.8}\mathrm{F}_{0.2}$ [Phys. Rev. B **83**, 174514 (2011)]. The magnetic field-temperature phase diagram of the mixed superconducting state is drawn for the three materials, displaying a sizable reduction of the liquid phase upon increasing T_c in the range of applied fields ($H \leqslant 5$ T). This result indicates that $\mathrm{SmFeAsO}_{0.8}\mathrm{F}_{0.2}$ is the most interesting compound among the investigated ones in view of possible applications. The field-dependence of the intragrain depinning energy U_0 exhibits a common trend for all the samples with a typical crossover field value (2500 Oe $\lesssim H_{\mathrm{cr}} \lesssim$ 5000 Oe) separating regions where single and collective depinning processes are at work.

DOI: 10.1103/PhysRevB.85.144522 PACS number(s): 74.25.Uv, 74.25.Wx, 74.70.Xa

I. INTRODUCTION

Almost four years after the discovery of high-temperature superconductivity in Fe-based pnictides,[1] several questions are still open both on fundamental aspects and on possible technological applications. No clear and exhaustive explanations for the precise pairing mechanism have been given yet. Incontrovertible features of isotopic effects cannot entirely rule out a partial role of the lattice in the coupling process,[2] but it is essential to stress that T_c's values are indeed too high to allow only a conventional pairing to be at work.[3] Strong evidences for a multiband s-wave scenario have been reported, together with theoretical support,[4,5] from a number of techniques in materials belonging to the 1111 family,[6–8] to 122 compounds,[9] and to 11 chalcogenides.[10]

At the same time, it is still not clear whether these novel compounds will be helpful as valid technological tools. The answer to these problems will essentially come from specific measurements of critical current densities in relation to the features of the grain boundaries. Detailed studies of the practical applicability of granular superconductors, anyway, cannot leave aside precise investigations of the fundamental intrinsic properties of the materials. In this respect, the determination of the so-called irreversibility line is of the utmost importance. Such a line, in fact, delimits the region in the magnetic field-temperature phase diagram where the dissipationless property of the thermodynamical superconducting phase is preserved even in the presence of a partial penetration of magnetic field inside the material. In a previous work on a powder sample of optimally doped $\mathrm{SmFeAsO}_{0.8}\mathrm{F}_{0.2}$ (see Ref. 11) the determination of the intrinsic irreversibility line was performed by means of the ac susceptibility technique. Parameters like the superconducting critical temperature T_c are, anyway, well known to be strongly dependent on the considered rare-earth (R) ion in 1111 oxypnictides.[12] The question of whether (and how) the properties of the phase diagram of the flux lines and of the relative irreversibility lines, too, are indeed dependent on the R ion is then of extreme importance.

In this paper, we report on the phase diagram of the flux lines in three powder samples of $R\mathrm{FeAsO}_{1-x}\mathrm{F}_x$ superconductors (R = La, Ce, Sm) under conditions of nearly optimal doping. In particular, much attention is devoted to the determination of the irreversibility line and its dependence on the R ion. The features of pinning mechanisms and, in particular, of the characteristic depinning energy barriers are investigated in detail within a thermally activated framework. Results are interpreted and analyzed by distinguishing two magnetic field regimes characterized by single and collective depinning processes. This allows us to make experimental data collapse on the same curve, a feature indicative of a common underlying mechanism independent on the precise material. A reliable estimate of the dependence of the anisotropy parameter γ on the R ion is finally given. Data relative to the Sm-based sample have already been presented in Ref. 11 and will be reported also here for the sake of clarity and completeness.

II. EXPERIMENTALS: ASPECTS OF DC MAGNETIZATION AND AC SUSCEPTIBILITY

Powder samples of $R\mathrm{FeAsO}_{1-x}\mathrm{F}_x$ (with R = La, Ce, Sm and nominal F^- contents $x = 0.1$, 0.08, and 0.2, respectively) were synthesized as described in previous works.[11,13–15] Static magnetization (M_{dc}) and ac susceptibility (χ_{ac}) measurements were performed by means of a Quantum Design MPMS-XL7 SQUID magnetometer and of a MPMS-XL5 SQUID susceptometer, respectively. In the latter case, a small alternating magnetic field H_{ac} with frequency ν_m is superimposed to a much higher static magnetic field H. Measurements were always performed in field-cooled (FC) conditions with H_{ac} = 0.0675–1.5 Oe parallel to $\mu_0 H$, which varied up to 5 T, while ν_m ranged from 37 to 1488 Hz.

M_{dc}/H versus temperature (T) raw data obtained under FC conditions at $H = 5$ Oe are shown in Fig. 1. For the sake of clarity, the curves have been reported after subtracting slight spurious contributions, leaving data above the superconducting onset at a constant zero offset value. $T_c(0)$ is defined as the critical temperature T_c for $H \to 0$ Oe. Such values are

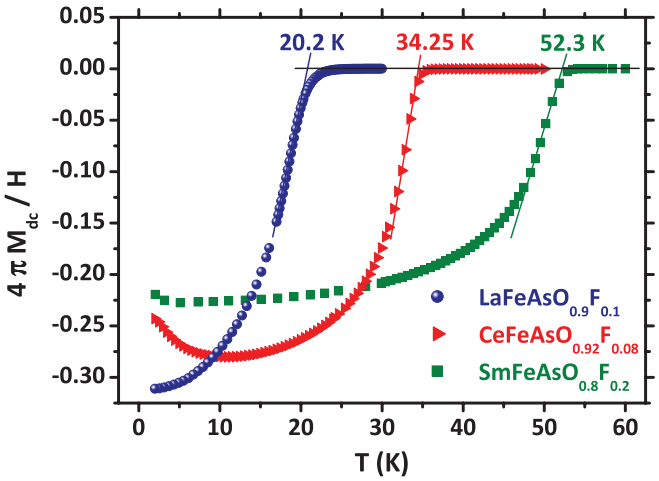

FIG. 1. (Color online) M_{dc}/H vs. T curves (volume units) in FC conditions at $H = 5$ Oe. The estimated $T_c(0)$ values are indicated in correspondence of the diamagnetic onsets.

obtained as the zero intercept of a linear extrapolation of the data below the diamagnetic onset[11] and reported in Fig. 1. The saturation absolute value of the diamagnetic signals is evaluated as (0.27 ± 0.05) in $1/4\pi$ units. These values are typical for fully superconducting powder samples in measurements under FC conditions, the observed reduction originating from the sample's geometrical properties and morphology. In the case of the $CeFeAsO_{0.92}F_{0.08}$ sample, a sizable paramagnetic contribution from the Ce sublattice can be clearly discerned already at such low value of magnetic field, mainly due to the high value of the Ce^{3+} magnetic moment. In fact, the fitting procedure to the experimental data at several values of H already described in a previous work[11] yields to $\mu_{Ce} \simeq 2.1\ \mu_B$ and $\mu_{Sm} \simeq 0.3\ \mu_B$ (raw data not shown).

Curves reported in Fig. 1 show quite sharp superconducting transitions. The slight roundness of the onset may be due to several reasons, both intrinsic (for instance the influence of superconducting fluctuations near T_c, as already discussed in Ref. 13) and extrinsic (slight chemical inhomogeneity of the F^- doping ions, distribution of the geometrical size of grains). The signal, moreover, comes from differently oriented grains in the powder sample and also this fact may contribute to a broadening of the transition at high-H values. The corresponding powder-averaged upper critical field

$$\langle H_{c2}(T)\rangle_{\rm pwd} \simeq \tfrac{2}{3} H_{c2,H\|ab}(T) + \tfrac{1}{3} H_{c2,H\|c}(T) \qquad (1)$$

was deduced for the three samples by examining the field dependence of T_c, as reported in Ref. 11.

In Fig. 2 some typical χ_{ac} versus T curves for $CeFeAsO_{0.92}F_{0.08}$ are displayed. Raw data of $SmFeAsO_{0.8}F_{0.2}$ have been reported previously,[11] while those for $LaFeAsO_{0.9}F_{0.1}$ are qualitatively similar to those in Fig. 2 and are not presented. The χ'_{ac} versus T curves can be described in terms of a mixed-state shielding response with some degree of distortion occurring in those T regions where sizable contributions to the imaginary component appear. χ''_{ac} versus T curves are composed of two main peaked contributions: a narrow peak appears just below the diamagnetic onset while a much broader one is present at low T. This is quite a common phenomenology in superconducting powder samples.[16,17] The high-T peak is generally associated with the power absorption due to losses inside the single grains, while the broad low-T peak can be associated with the generation of weak Josephson-like links among the different grains.

The three main features shown in Fig. 2, namely the diamagnetic onset in χ'_{ac} and the two peaks in χ''_{ac}, are strongly shifted to lower T on increasing H for all the samples. The H dependence of the diamagnetic onset in χ'_{ac}, in particular, is much more marked than in the case of the diamagnetic onset in M_{dc}/H versus T curves. The described behavior can be directly associated to vortex dynamics. The precise features of the irreversibility line, in fact, can be obtained by considering the intrinsic dissipative response inside the grains.[11,18–25] In particular, by examining the χ''_{ac} versus T curves, one can denote by T_p the position of the intragrain maximum, which

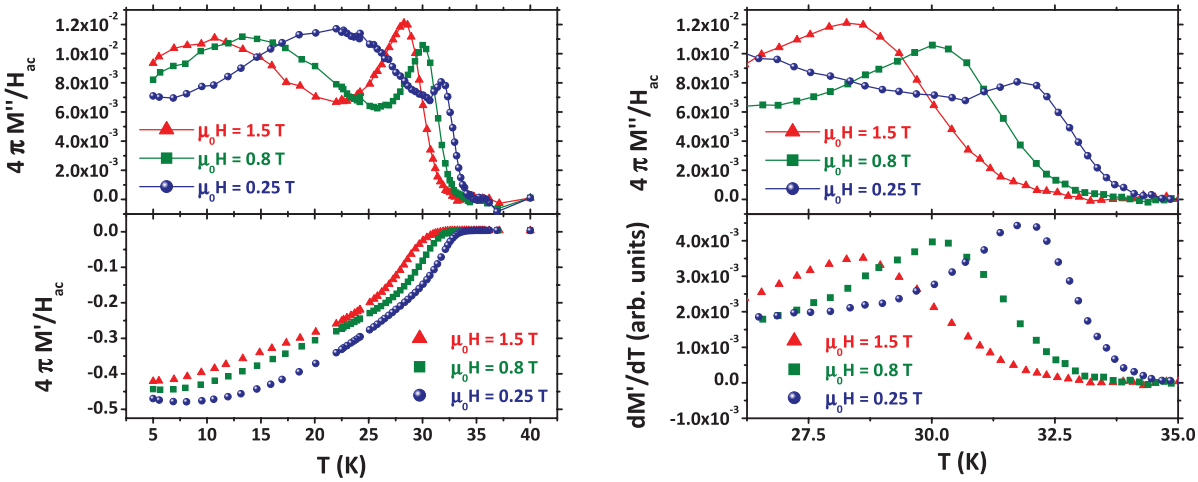

FIG. 2. (Color online) Left: χ_{ac} vs. T raw data for $CeFeAsO_{0.92}F_{0.08}$ ($H_{ac} = 1.5$ Oe and $\nu_m = 478$ Hz) at different H values. The imaginary and the real components are shown in the upper and lower panels, respectively (volume units). Right: zoom of the onset region of the curves already reported in the left panels relative to χ''_{ac} and to the first derivative of χ'_{ac} with respect to T (upper and lower panels, respectively. See text for further details).

is typically found just a few K below the diamagnetic onset in χ'_{ac}. This peak can be interpreted as arising from a resonating absorption of energy when the frequency of the radiation matches the inverse characteristic relaxation time $1/\tau_c$ of the vortices in the pinning potential dip, namely,

$$2\pi \nu_m \tau_c|_{T=T_p} = 1. \quad (2)$$

The H dependence of T_p can then be chosen in order to describe the irreversibility line and in the following we will be referring to this as the χ''_{ac} criterion. Within a Debye-like relaxation framework, T_p almost coincides with the characteristic temperature of the corresponding peak in the derivative of χ'_{ac} with respect to T. This was experimentally verified in all the three investigated samples,[11] as explicitly shown only in the case of $CeFeAsO_{0.92}F_{0.08}$ in the right panel of Fig. 2.

III. PHASE DIAGRAMS AND DEPINNING ENERGY BARRIERS: MAIN RESULTS

The FLs phase diagrams for the three samples are shown in Fig. 3 where both $\langle H_{c2}(T)\rangle_{pwd}$ (full symbols) and the irreversibility lines (open symbols) are plotted as a function of the reduced temperature $t \equiv T/T_c(0)$.

$\langle H_{c2}(T)\rangle_{pwd}$ versus t curves as determined from M_{dc} data clearly display linear trends as a function of t. At low-t values, anyway, a slight upper curvature can be detected for all the samples, a feature possibly associated with two-band superconductivity.[26] Data relative to $CeFeAsO_{0.92}F_{0.08}$ are limited to the low-H values due to the dominant paramagnetic contribution arising from the Ce^{3+} sublattice, which fully covers the superconducting response for $\mu_0 H \gtrsim 2$ T. The slope of a linear fit to the data allows us to estimate the upper critical field $\langle H_{c2}(0)\rangle_{pwd}$ extrapolated at $T = 0$ K under the simplified assumption of single-band s-wave superconductivity through

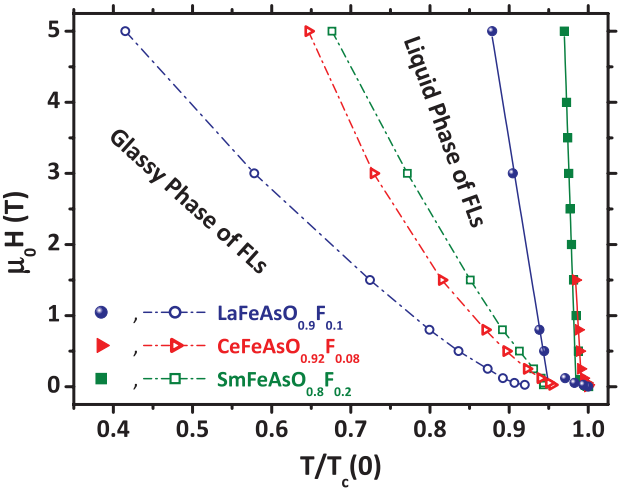

FIG. 3. (Color online) Phase diagrams for the FLs in the investigated samples. Data for $SmFeAsO_{0.8}F_{0.2}$ have already been reported in Ref. 11. Open symbols track the irreversibility line as deduced from data taken at $\nu_m = 37$ Hz (dashed-dotted lines are guides for the eye). Full symbols track $\langle H_{c2}(T)\rangle_{pwd}$ (continuous lines are linear fits).

TABLE I. Critical temperature $T_c(0)$ for $H \to 0$ Oe and correlation length $\langle\xi(0)\rangle_{pwd}$ for $T \to 0$ K as deduced from Eqs. (3) and (4).

Sample	$T_c(0)$ (K)	$\langle\xi(0)\rangle_{pwd}$ (Å)
$SmFeAsO_{0.8}F_{0.2}$	52.3 ± 0.25	11.0 ± 0.1
$CeFeAsO_{0.92}F_{0.08}$	34.25 ± 0.25	15.7 ± 0.3
$LaFeAsO_{0.9}F_{0.1}$	20.2 ± 0.25	26.3 ± 0.5

the relation

$$\langle H_{c2}(0)\rangle_{pwd} \simeq 0.7 \times T_c(0) \left|\frac{d\langle H_{c2}\rangle_{pwd}}{dT}\right|_{T\simeq T_c(0)}, \quad (3)$$

following from the so-called WHH approach.[27] From the relation[28,29] (see Table I)

$$\langle H_{c2}(0)\rangle_{pwd} \equiv \frac{\Phi_0}{2\pi\langle\xi(0)\rangle^2_{pwd}}, \quad (4)$$

an overall correlation is observed between the gradual increase of $T_c(0)$ and a steady decrease of the extrapolated value of the powder-averaged Ginzburg-Landau (GL) coherence length $\langle\xi(0)\rangle_{pwd}$ at $T = 0$ K.

Results from χ_{ac} data will now be considered. The χ''_{ac} criterion was chosen for the determination of the irreversibility line. Data relative to the derivative of χ'_{ac} were always analyzed due to their more favorable signal-to-noise ratio. A slight dependence of the T_p value on ν_m was detected for all the H values. For this reason, data for the lowest accessible value $\nu_m = 37$ Hz were chosen in order to draw the irreversibility lines in Fig. 3. The extension of the liquid phase of the flux lines is progressively reduced by the increase of T_c in the explored H range. This observation, together with the estimate of the high value of the intrinsic critical current density,[11] makes Sm-based materials rather interesting in view of possible technological applications.

In order to better compare the behavior of the three samples from a fundamental point of view, the irreversibility lines reported in Fig. 3 are presented again in Fig. 4 after normalizing the field values by $\langle H_{c2}(0)\rangle_{pwd}$. In all three samples the irreversibility line can be described by means of a power-law function,

$$\frac{H}{\langle H_{c2}(0)\rangle_{pwd}} \propto \left[(1-\varepsilon) - \frac{T}{T_c(0)}\right]^{\beta}, \quad (5)$$

characterized by the exponent $\beta = 3/2$ (see the continuous lines in Fig. 4). This is a typical result in high-T_c superconductors,[11,18,30] even if slightly different functional form have been reported, for instance, in the case of $Ba(Fe_{1-x}Co_x)_2As_2$ single crystals.[31] Here, the coefficient $\varepsilon \simeq 0.05$ (common for all the samples) phenomenologically accounts for the discrepancies at low-H values when defining the irreversibility line from the χ''_{ac} criterion. It should be noticed that, after the proper normalization of both the T- and H-axes, the extension of the liquid phase as a function of the R ion shows a trend opposite to what is displayed in Fig. 3. This interesting feature will be recalled and discussed later in Sec. IV.

One can notice that, similarly to what was observed in $SmFeAsO_{0.8}F_{0.2}$,[11] the quantity $1/T_p$ displays a logarithmic

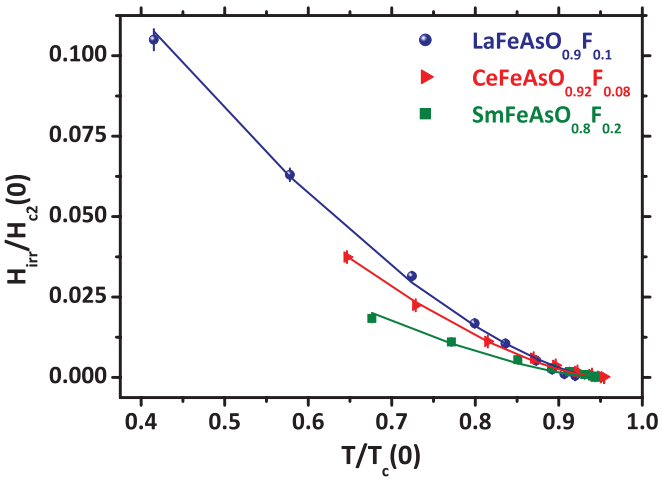

FIG. 4. (Color online) Representation of the irreversibility lines relative to the investigated samples [already reported in the phase diagrams (see Fig. 3)], where $H_{\rm irr}(T)$ has been normalized with respect to the relative value of $\langle H_{c2}(0)\rangle_{\rm pwd}$. Continuous lines are best fits according to Eq. (5).

dependence on ν_m. This is clearly shown in the inset of Fig. 5 for $CeFeAsO_{0.92}F_{0.08}$ ($H_{\rm ac} = 1.5$ Oe, $\mu_0 H = 1.5$ T), even if the phenomenology is well verified for all the samples at all the H values. In particular, data can always be fitted within a thermally activated framework by the expression

$$\frac{1}{T_p(\nu_m)} = -\frac{1}{\langle U_0(H)\rangle_{\rm pwd}} \ln\left(\frac{\nu_m}{\nu_0}\right) \qquad (6)$$

(see the fitting function in the inset of Fig. 5). The logarithmic behavior of $1/T_p$ is controlled by the powder-averaged parameter $\langle U_0(H)\rangle_{\rm pwd}$, playing the role of an effective depinning energy barrier in a thermally activated flux creep model. The parameter ν_0 in Eq. (6) represents an intravalley characteristic

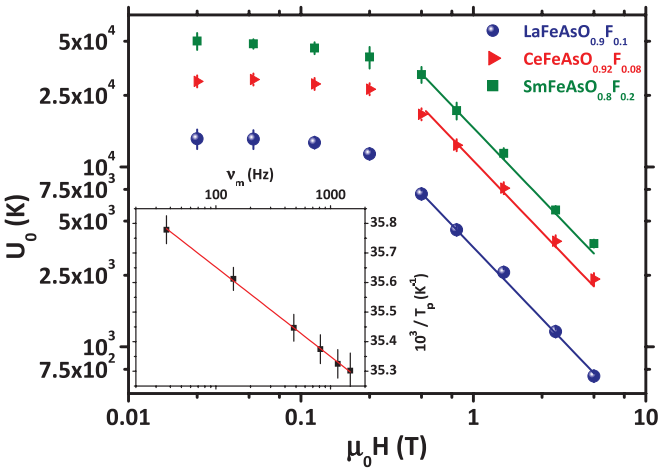

FIG. 5. (Color online) Main panel: H dependence of the depinning energy barriers $\langle U_0(H)\rangle_{\rm pwd}$ in the three investigated samples. Data relative to $SmFeAsO_{0.8}F_{0.2}$ have already been reported in a previous work.[11] Continuous lines are best-fits to data according to a simple $1/H$ dependence. Inset: logarithmic ν_m dependence of $1/T_p$ in $CeFeAsO_{0.92}F_{0.08}$ ($H_{\rm ac} = 1.5$ Oe while $\mu_0 H = 1.5$ T). The continuous line is a best-fit function according to Eq. (6).

frequency associated with the motion of the vortices around their equilibrium position in the pinning centers.

The results of the fitting procedure to T_p (ν_m) data according to Eq. (6) have been reported in the main panel of Fig. 5 for all the samples. A strongly marked H dependence of $\langle U_0(H)\rangle_{\rm pwd}$ common to all the samples can clearly be discerned. Beyond an overall sizable reduction of $\langle U_0(H)\rangle_{\rm pwd}$ with increasing H, a sharp crossover (at field values 2500 Oe $\lesssim H_{\rm cr} \lesssim$ 5000 Oe common to all the samples) between two qualitatively different $\langle U_0(H)\rangle_{\rm pwd}$ versus H regimes is observed. At low fields, $H < H_{\rm cr}$, the depinning energy $\langle U_0(H)\rangle_{\rm pwd}$ is found to be only slightly dependent on H, while for values $H > H_{\rm cr}$ a trend $\langle U_0(H)\rangle_{\rm pwd} \propto 1/H$ can be discerned. The $1/H$ regime for depinning energies $\langle U_0(H)\rangle_{\rm pwd}$ was indeed observed in different superconducting materials by means of several techniques ranging from magnetoresistivity[23] to ac magnetometry itself[24] and nuclear magnetic resonance.[32] This feature has already been reported in the $SmFeAsO_{0.8}F_{0.2}$ sample[11] and, as it will be discussed later on, it can be justified in terms of pinning effects on a single FL propagating among bundles of entangled FLs. In this framework, the crossover between the two different trends of $\langle U_0(H)\rangle_{\rm pwd}$ versus H shown in Fig. 5 can be interpreted as the transition from a basically single-flux line response at low H values to a collective response of vortices for $H > 5000$ Oe. The saturated low-H values for the depinning energy barriers are typically $\langle U_0(H)\rangle_{\rm pwd} \sim 10^4$ K. Such high values are in agreement with those reported from magnetoresistivity measurements in $SmFeAsO_{0.85}$ (see Ref. 33) and in $Ba_{1-x}K_xFe_2As_2$ single crystals, even if in the latter case a much weaker H dependence was observed.[34] These results are clearly indicative of strong intrinsic pinning of the vortex lines, in agreement with what deduced in single-crystals of $PrFeAsO_{1-x}$ and $NdFeAsO_{1-x}F_x$, confirming that the observed behavior is intrinsic in $RFeAsO_{1-x}F_x$ materials.[35] It should be remarked that a similar $1/H$ dependence for the depinning energy barriers was observed in Tm-based cuprate materials and interpreted following scaling arguments concerning the magnetization curves.[36]

It must be observed that, since the variation of T_p versus ν_m is very modest (see the vertical scale in the inset of Fig. 5), $\langle U_0(H)\rangle_{\rm pwd}$ is not only determined at a fixed H but in almost-isothermal conditions as well. Correspondingly, one can notice that, according to the $\chi''_{\rm ac}$-criterion, the average temperature T^* characterizing the variation of T_p over the considered ν_m range is essentially positioned over the irreversibility line. This holds for all the corresponding H^* values of magnetic field, so that the energy barrier will be referred to as $\langle U_0(H^*, T^*)\rangle_{\rm pwd}$.

IV. ANALYSIS OF THE RESULTS AND DISCUSSION

The observed behavior can be explained by means of the phenomenological GL theory within a simple two-fluids approximation[28] and by referring to the model of single-vortex pinning by atomic impurities (such as, for instance, ionic substitutions like O^{2-}/F^- or O^{2-} vacancies).[18,19,30] Due to the very small values of the coherence lengths $\sim$10 Å, in fact, local defects on the atomic scale can be considered as strongly efficient pinning centers for FLs.[33] In this framework, the energy U_0 is related to the FLs features only and does not depend on the precise pinning mechanisms.[19] Moreover, at

strong H values the high density of FLs gives rise to entangled bundles of vortices around the central one physically bound to the atomic defect.[18,19,30] Accordingly, the characteristic energy U_0 can be directly linked to the geometrical properties of the flux line lattice and, in particular, to the typical volume V of the correlated vortex lines. The following phenomenological expression can be envisaged (where U_0 is expressed in K):[18,19,30]

$$U_0(T) = \left\{ \frac{H_c^2(T)}{8\pi} \right\} \frac{V}{k_B}, \tag{7}$$

where the term between curly brackets quantifies the T dependence of the superconducting condensation energy density.

The characteristic volume V turns out to be strongly dependent on the geometrical features of the FLs that, in turn, are sizeably sensitive to the value of the externally applied magnetic field H. By considering the range of variability of H, then, two limiting cases can be described. On the one hand, by gradually increasing H the density of vortices steadily increases and, accordingly, correlations among vortices increase too. A crossover to a regime where the depinning process leads to a collective response of an increasing number of vortices is then expected. In the simplified scenario of a square Abrikosov lattice of vortices, the quantity $d = \sqrt{\Phi_0/H}$ estimates the mutual distance among nearest neighboring FLs. One can then assume that the correlations roughly extend over a cylindric volume whose radius is given by d. Namely, one has $V \simeq \pi\xi(T)\Phi_0/H$, the characteristic size along the third dimension being determined by the coherence length (even if different alternatives have been considered in literature).[30] After the substitution in Eq. (7), considerations on the powder-averaging make it possible to obtain a more convenient form in order to describe the present experimental data. In particular, the following relation holds (see Appendix A1 for details)

$$\langle U_0(H^*,T^*)\rangle_{\rm pwd} = \frac{\Phi_0^{5/2}}{96\sqrt{2}\pi^{3/2}k_B} \frac{g(t^*)\sqrt{\langle H_{c2}(0)\rangle_{\rm pwd}}}{H^*} \times \frac{1}{f_1(\gamma)\lambda_{\rm ab}^2(0)}, \tag{8}$$

where $g(t)$ is a function of t and $f_1(\gamma)$ is a function of the anisotropy parameter $\gamma = \xi_{\rm ab}/\xi_c = \lambda_c/\lambda_{\rm ab}$.

On the other hand, at low enough H values the typical volume V will be no longer sensitive to the presence of several flux lines but it will only be a function of the typical lengths of the single pinned vortex. As a consequence, one can consider a different cylindric volume with radius $\delta\xi(T)$. Here, the heuristic parameter δ is introduced in order to grant a continuous crossover between the high- and the low-H regimes.[30] Thus, again choosing $\xi(T)$ as the characteristic size also along the third dimension, the following relation holds:

$$\langle U_0(H^*,T^*)\rangle_{\rm pwd} = \frac{\Phi_0^{5/2}\delta^2}{192\sqrt{2}\pi^{5/2}k_B} \frac{h(t^*)}{\sqrt{\langle H_{c2}(0)\rangle_{\rm pwd}}} \times \frac{1}{f_2(\gamma)\lambda_{\rm ab}^2(0)}. \tag{9}$$

Here, $h(t)$ is a function of t and $f_2(\gamma)$ is a function of the anisotropy parameter (details relative to the derivation of Eq. (9) can be found in Appendix A2).

The two resulting expressions show that in both the H regimes $\lambda_{\rm ab}(0)$ can be simply expressed as a function of the experimentally accessible quantity $\langle U_0(H^*,T^*)\rangle_{\rm pwd}$. One should consider that the continuity of $\lambda_{\rm ab}(0)$ must clearly be assured at the crossover field.[30] The free parameters for the three different samples (namely, the anisotropy parameter γ_R and the parameter δ_R), anyway, make the fulfillment of this requirement quite arbitrary. Some other criterion from the analysis of experimental data should be formulated in order to derive some relations among the parameters, reducing as much as possible the degree of arbitrariness. This can be done by the examination of the FLs phase diagram and by taking into consideration the role of thermal fluctuations. As a final result of the procedure, as reported in detail in Appendix B, one finds that

$$\gamma_{\rm Sm}^{3/2}\delta_{\rm Sm}^2 \simeq 1.6\gamma_{\rm Ce}^{3/2}\delta_{\rm Ce}^2 \simeq 3\gamma_{\rm La}^{3/2}\delta_{\rm La}^2. \tag{10}$$

As a starting point of the described procedure, a reasonable value for one of the γ_R parameters should be taken as fixed. By referring to typical data reported in the literature,[37] in particular, it will be assumed that $\gamma_{\rm Sm} = 5$. Next, data relative to the two different regimes (high and low H) in $SmFeAsO_{0.8}F_{0.2}$ are linked up by setting a proper value of $\delta_{\rm Sm}$. The procedure is repeated also for Ce- and La-based samples, where the starting guesses for the parameters γ_R and δ_R must be modified till the fulfillment of Eq. (10). The values obtained for both γ_R and δ_R after such procedure have been reported in Table II. The observed behavior of δ as a function of the R ion can be qualitatively understood in terms of a compensation of the opposite trend in $\langle\xi\rangle_{\rm pwd}$. The trend in the modification of the value of γ, on the other hand, can be correlated with the increase in the size of the liquid region in the phase diagram reported in Fig. 4. One can deduce that the increase in γ possibly leads to the enhancement of two-dimensional fluctuations, much more effective than the higher-dimensional ones in extending the liquid region of the phase diagram. It should be remarked that a similar trend of γ in La- and Sm-based samples was reported in literature, even if the measured absolute values were considerably higher.[38]

It should be stressed that the linking procedure allows one to enlighten a scaling of data over the entire H range, as reported in Fig. 6. After a proper normalization with respect to the value $\lambda_{\rm ab}^{-2}(0)$ taken at $H = 250$ Oe, in fact, a clearly common H dependence can be discerned independently on the examined sample. This feature possibly demonstrates the existence of a common material-independent underlying mechanism. The estimates of $\lambda_{\rm ab}(0)$ in the $H \to 0$ Oe limit for $CeFeAsO_{0.92}F_{0.08}$ and $SmFeAsO_{0.8}F_{0.2}$ are consistent with the values obtained from μ^+SR measurements on the same

TABLE II. Parameters δ and γ for the three samples resulting from the constrained linking procedure of data relative to the two distinct H regimes (see text for details).

Sample	γ	δ
$LaFeAsO_{0.9}F_{0.1}$	3.2	9.5
$CeFeAsO_{0.92}F_{0.08}$	4.25	10.5
$SmFeAsO_{0.8}F_{0.2}$	5	11.75

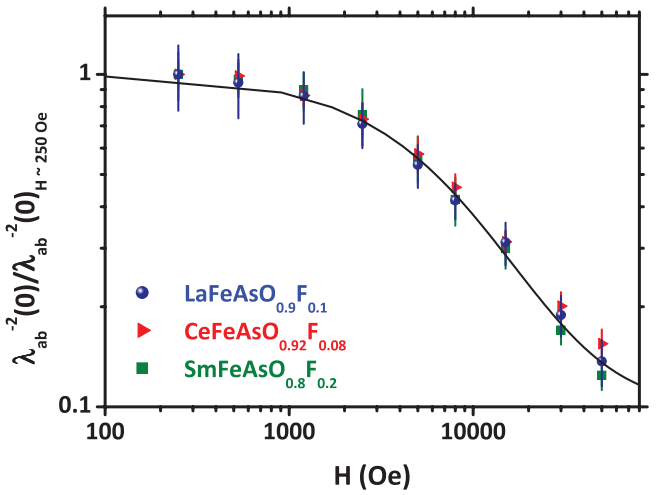

FIG. 6. (Color online) Graphical representation of the collapse of experimental data represented in Fig. 5 after a proper normalization according to the value of $1/\lambda_{ab}^2(0)$ estimated at 250 Oe. The continuous line is a guide to the eye.

samples (unpublished data) within a factor ∼2. This is confirmed by a comparison with μ^+SR data on different samples characterized by slightly different stoichiometries (see Refs. 39 and 40). This discrepancy can be justified in terms of the high degree of arbitrariness associated with the choice of the correlation volumes V in the two different H regimes or, possibly, with the too-rough two-fluid approximation employed for modeling the T-dependence of the typical length scales. The factor ∼2 is, anyway, constant and well verified for the three samples, strongly hinting at the substantial correctness of the procedure even if the presence of a systematic source of error is assumed.

V. CONCLUSIONS

The phase diagram of the flux lines in three powder samples of RFeAsO$_{1-x}$F$_x$ superconductors (R = La, Ce, Sm) under conditions of nearly optimal doping was investigated by means of ac susceptibility measurements. The irreversibility line has been estimated for the three samples, showing that in the accessible range of magnetic field the extension of the reversible liquid region is lowered with increasing T_c. This aspect could be of extreme interest in view of possible technological applications of these materials. The H dependence of the characteristic depinning energy barriers was investigated in a thermally activated framework. Results were interpreted by distinguishing two regimes of magnetic field characterized by single and collective depinning processes, allowing us to make experimental data collapse on the same magnetic field trend indicative of a common underlying mechanism independent on the precise material.

ACKNOWLEDGMENTS

R. Khasanov, G. Lamura, and A. Rigamonti are gratefully acknowledged for stimulating discussions. H. Stummer, C. Malbrich, S. Müller-Litvanyi, R. Müller, K. Leger, J. Werner, and S. Pichl are acknowledged for assistance in the sample preparation. The work at the IFW Dresden was supported by the Deutsche Forschungsgemeinschaft through Grant No. BE1749/12 the Priority Program SPP1458 (Grant No. BE1749/13). S.W. acknowledges support by DFG under the Emmy-Noether Program (Grant No. WU595/3-1).

APPENDIX A: DERIVATION OF THE RELATIONS BETWEEN $\langle U_0(H^*,T^*)\rangle_{pwd}$ AND $\lambda_{ab}(0)$ IN THE TWO DIFFERENT H REGIMES

1. Strongly correlated vortices: Depinning of bundles of flux lines

Let's consider Eq. (7) in the limit of high H, here rewritten for convenience

$$U_0(H,T) = \frac{H_c^2(T)}{8k_B}\frac{\xi(T)\Phi_0}{H}, \tag{A1}$$

as the starting point. By means of the GL relation for the flux quantum $\Phi_0 = 2\sqrt{2}\pi H_c(T)\lambda(T)\xi(T)$, one can write down an explicit expression for U_0 in different conditions of orientation of the magnetic field as follows

$$U_{0,H\|ab}(H,T) = \frac{\Phi_0^3}{64\pi^2 k_B H}\frac{1}{\sqrt{\xi_{ab}(T)\xi_c(T)}\lambda_{ab}(T)\lambda_c(T)}$$
$$U_{0,H\|c}(H,T) = \frac{\Phi_0^3}{64\pi^2 k_B H}\frac{1}{\xi_{ab}(T)\lambda_{ab}^2(T)}. \tag{A2}$$

The expressions $\xi_{ab}/\xi_c = \lambda_c/\lambda_{ab} = \gamma$ hold for the different typical lengths in anisotropic superconductors, where γ has already been defined in the text as the anisotropy parameter. By referring to Eq. (1), it is possible to perform a powder-like average of U_0 as

$$\langle U_0(H,T)\rangle_{pwd} \equiv \frac{2}{3}U_{0,H\|ab}(T) + \frac{1}{3}U_{0,H\|c}(T)$$
$$= \left(\frac{\sqrt{\gamma}+2}{3\gamma^{3/2}}\right)\frac{\Phi_0^3}{64\pi^2 k_B H}\frac{1}{\xi_c(T)\lambda_{ab}^2(T)}. \tag{A3}$$

In a simple two-fluid model, the T-dependence of $\xi_c(T)$ and $\lambda_{ab}(T)$ can be taken as

$$\xi_c(T) = \xi_c(0)\frac{\sqrt{1-t^4}}{1-t^2}, \quad \lambda_{ab}(T) = \lambda_{ab}(0)\frac{1}{\sqrt{1-t^4}}, \tag{A4}$$

where t has already been defined as the reduced temperature $t \equiv T/T_c(0)$. It should be considered that, as already recalled, the estimate of $\langle U_0(H,T)\rangle_{pwd}$ is performed by definition at the values (H^*,T^*) delimiting the irreversibility line. After the definition of the function $g(t) \equiv (1-t^2)\sqrt{1-t^4}$, it is then possible to write

$$\frac{\langle U_0(H^*,T^*)\rangle_{pwd}}{g(t^*)} = \left(\frac{\sqrt{\gamma}+2}{3\gamma^{3/2}}\right)\frac{\Phi_0^3}{64\pi^2 k_B H^*}\frac{1}{\xi_c(0)\lambda_{ab}^2(0)}. \tag{A5}$$

The quantity $\xi_c(0)$ can be independently derived by measuring the magnetic field dependence of the superconducting transition temperature T_c by means of the relations reported in Eqs. (3) and (4) after proper considerations about the powder-average procedures. The two limiting configurations

$H \parallel$ ab and $H \parallel c$ lead to the formulas

$$H_{c2,H\parallel ab}(T) = \frac{\Phi_0}{2\pi\xi_{ab}(T)\xi_c(T)},$$
$$H_{c2,H\parallel c}(T) = \frac{\Phi_0}{2\pi\xi_{ab}^2(T)}. \quad \text{(A6)}$$

Following Eq. (1), it is possible to deduce that the experimentally accessible quantity $\langle\xi(0)\rangle_{pwd}$, already defined in Eq. (4), is linked to $\xi_c(0)$ by the relation

$$\langle\xi(0)\rangle_{pwd} = \xi_c(0)\left(\frac{\sqrt{3}\gamma}{\sqrt{2\gamma+1}}\right). \quad \text{(A7)}$$

Coming back to Eq. (A5), one can substitute Eqs. (A7) and (4) to obtain

$$\frac{\langle U_0(H^*,T^*)\rangle_{pwd}}{g(t^*)\sqrt{\langle H_{c2}(0)\rangle_{pwd}}} = \frac{\Phi_0^{5/2}}{96\sqrt{2}\pi^{3/2}k_B}\frac{1}{f_1(\gamma)\lambda_{ab}^2(0)}\frac{1}{H^*}, \quad \text{(A8)}$$

having defined the function of the anisotropy parameter

$$f_1(\gamma) = \frac{1}{\sqrt{3}}\frac{\sqrt{2\gamma^2+\gamma}}{\sqrt{\gamma}+2}. \quad \text{(A9)}$$

Eq. (A8) is equivalent to Eq. (8).

2. Weakly correlated vortices: Depinning of single flux lines

Let's now consider Eq. (7) in the limit of low H, here rewritten for convenience

$$U_0(T) = \frac{H_c^2(T)}{8k_B}\delta^2\xi^3(T). \quad \text{(A10)}$$

Again, by means of the GL relation for the flux quantum $\Phi_0 = 2\sqrt{2}\pi H_c(T)\lambda(T)\xi(T)$, it is possible to explicit the expressions for U_0 in the different cases of the orientation of the system with respect to the magnetic field as

$$U_{0,H\parallel ab}(T) = \frac{\Phi_0^2\delta^2}{64\pi^2k_B}\frac{\sqrt{\xi_{ab}(T)\xi_c(T)}}{\lambda_{ab}(T)\lambda_c(T)}$$
$$U_{0,H\parallel c}(T) = \frac{\Phi_0^2\delta^2}{64\pi^2k_B}\frac{\xi_{ab}(T)}{\lambda_{ab}^2(T)}. \quad \text{(A11)}$$

Similarly to what performed in the previous appendix concerning strongly correlated vortices, the γ factor can be introduced and $\lambda_{ab}(T)$, $\xi_c(T)$ can be left as independent quantities. By considering that the estimate of $\langle U_0(H,T)\rangle_{pwd}$ is performed along the irreversibility line (H^*,T^*), by employing Eq. (A4) and after a powder-like average of the energy barrier, one can write

$$\frac{\langle U_0(H^*,T^*)\rangle_{pwd}}{h(t^*)} = \left(\frac{\gamma^2+2\sqrt{\gamma}}{3\gamma}\right)\frac{\Phi_0^2\delta^2}{64\pi^2k_B}\frac{\xi_c(0)}{\lambda_{ab}^2(0)}, \quad \text{(A12)}$$

where $h(t) \equiv (1+t^2)\sqrt{1-t^4}$. By again expressing $\xi_c(0)$ in terms of $\langle H_{c2}(0)\rangle_{pwd}$ through Eq. (A7) and by means of Eq. (4), it is finally possible to deduce the following expression:

$$\frac{\langle U_0(H^*,T^*)\rangle_{pwd}\sqrt{\langle H_{c2}(0)\rangle_{pwd}}}{h(t^*)} = \frac{\Phi_0^{5/2}\delta^2}{192\sqrt{2}\pi^{5/2}k_B} \times \frac{1}{f_2(\gamma)\lambda_{ab}^2(0)}. \quad \text{(A13)}$$

In the previous expression, $f_2(\gamma)$ is defined as

$$f_2(\gamma) = \frac{\sqrt{3}\gamma^2}{(\gamma^2+2\sqrt{\gamma})\sqrt{2\gamma+1}}. \quad \text{(A14)}$$

Eq. (A13) is equivalent to Eq. (9).

APPENDIX B: LINKING PROCEDURE OF DATA IN THE TWO DIFFERENT H REGIMES

In this Appendix, the problem of the continuity at the crossover field H_{cr} of the $\lambda_{ab}(0)$ versus H data, obtained by means of Eqs. (8) and (9), will be considered. In particular, as already stated in the text, some constraints on the variability of the six parameters γ_R and δ_R (R = La, Ce, Sm) should be fixed in order to reduce as much as possible the degree of arbitrariness of the procedure of data-linking.

At this aim, it is convenient to introduce the Ginzburg-Levanyuk number $\widetilde{Gi}_{3D}(0)$ as[41]

$$\widetilde{Gi}_{3D}(0) = \frac{1}{2}\left[\frac{8\pi^2k_BT_c(0)\lambda^2(0)}{\Phi_0^2\xi(0)}\right]^2, \quad \text{(B1)}$$

quantifying the extension of the region of the $H-T$ phase diagram, where thermal fluctuations are sizable and significantly affect the physics of the system. The H dependence of $\widetilde{Gi}_{3D}(0)$ is given by[41]

$$Gi_{3D}(0,H) = \left[\frac{2H\sqrt{\widetilde{Gi}_{3D}(0)}}{H_{c2}(0)}\right]^{2/3}. \quad \text{(B2)}$$

In fact, one can assume that the position of the irreversibility line is mainly governed by the amount of thermal fluctuations in the system. As a consequence, $Gi_{3D}(0,H)$ is expected to be directly involved in the analytic expression relative to the irreversibility line itself. One hint at the correctness of this picture is possibly given by the similarity between the characteristic exponents observed in Eqs. (5) and (B2). Similar considerations, moreover, have already been proposed in literature concerning the thermodynamical melting line (see, in particular, Secs. IV and V of Ref. 42 and references therein. In that case, anyway, the considered exponent is $\beta = 2$). The following expression for the irreversibility line can then be considered

$$1 - \frac{T^*}{T_c(0)} = \frac{Gi_{3D}(0,H^*)}{K^{2/3}}, \quad \text{(B3)}$$

where K is an arbitrary proportionality factor. Together with Eq. (B2), this straightforwardly leads to

$$\frac{2H^*\sqrt{\widetilde{Gi}_{3D}(0)}}{H_{c2}(0)} = K\left[1-\frac{T^*}{T_c(0)}\right]^{3/2}. \quad \text{(B4)}$$

Since all the sample-dependent quantities are already kept into consideration by $\widetilde{Gi}_{3D}(0)$, it is reasonable to assume K as a sample-independent parameter. K can typically be interpreted

in terms of microscopic properties of the vortices.[42] In the present phenomenological model, anyway, such microscopic interpretations are left aside.

In order to give a suitable description of the experimental data, Eq. (B4) should be powder-averaged by considering the criterion already presented in Eq. (1). By considering the definition of $\widetilde{Gi}_{3D}(0)$ reported in Eq. (B1), one can write

$$\frac{\sqrt{\widetilde{Gi}_{3D}(0)}}{H_{c2}(0)} = \frac{1}{\sqrt{2}} \frac{8\pi^2 k_B T_c(0)\lambda_{ab}(0)\lambda_c(0)}{\Phi_0^2\sqrt{\xi_{ab}(0)\xi_c(0)}} \frac{2\pi\xi_{ab}(0)\xi_c(0)}{\Phi_0}$$
$$\frac{\sqrt{\widetilde{Gi}_{3D}(0)}}{H_{c2}(0)} = \frac{1}{\sqrt{2}} \frac{8\pi^2 k_B T_c(0)\lambda_{ab}^2(0)}{\Phi_0^2\xi_{ab}(0)} \frac{2\pi\xi_{ab}^2(0)}{\Phi_0} \qquad \text{(B5)}$$

for the two field orientations $H \parallel$ ab and $H \parallel c$, respectively. By again performing the powder-average procedure and after introducing the anisotropy parameter through the relations $\xi_{ab}/\xi_c = \lambda_c/\lambda_{ab} = \gamma$, by referring to Eqs. (4) and (A7), one obtains the following expression:

$$\left\langle \frac{\sqrt{\widetilde{Gi}_{3D}(0)}}{H_{c2}(0)} \right\rangle_{pwd} = \frac{1}{f_3(\gamma)} \frac{8\pi^2 k_B T_c(0)\lambda_{ab}^2(0)}{\sqrt{2}\Phi_0^2\xi_c(0)} \frac{1}{\langle H_{c2}(0)\rangle_{pwd}}, \qquad \text{(B6)}$$

where the function $f_3(\gamma)$ is defined as

$$f_3(\gamma) = \frac{9\gamma^2}{\left(2\gamma^{3/2}+\gamma\right)(2\gamma+1)}. \qquad \text{(B7)}$$

One should now consider that the definition of $\widetilde{Gi}_{3D}(0)$ reported in Eq. (B1) does not account for any H dependence that is fully accounted for by Eq. (B2). Equation (B6) is then referred to a $H = 0$ Oe condition and, as a consequence, the quantity $\lambda_{ab}^2(0)/\xi_c(0)$ can be obtained by means of Eq. (A12) (holding in the low-H regime). By inserting the resulting expression into Eq. (B4), one obtains

$$\frac{H^*}{\langle H_{c2}(0)\rangle_{pwd}} \simeq \widetilde{K}_R \times \left[0.95 - \frac{T^*}{T_c(0)}\right]^{3/2}, \qquad \text{(B8)}$$

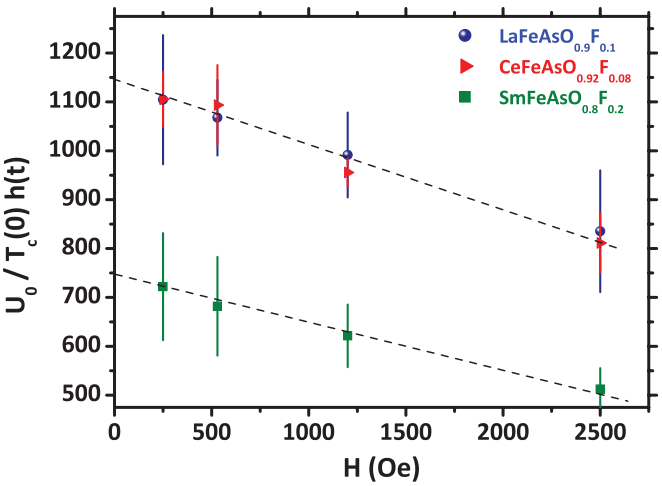

FIG. 7. (Color online) Graphical representation of the quantity between curly brackets in Eq. (B9). The dashed lines are guides for the eye and they can be used to extrapolate the intercept values back to $H = 0$ Oe.

where

$$\widetilde{K}_R \equiv \left\{ \frac{\langle U_0(H^*,T^*)\rangle_{pwd}}{T_c(0)h(t^*)} \right\}_R \times \frac{27\sqrt{2}}{\gamma_R^{3/2}\delta_R^2} K. \qquad \text{(B9)}$$

As already discussed in the text, the factor 0.95 in Eq. (B8) phenomenologically accounts for the definition of the irreversibility line from the χ''_{ac} criterion.

The quantity between curly brackets in Eq. (B9) can be experimentally estimated from a linear extrapolation of the intercept values back to $H = 0$ Oe (see Fig. 7). One can then compare the sample-dependent quantity $\widetilde{K}_R$ with the corresponding experimental quantities derived from the fitting procedure shown in Fig. 4. Together with the already cited assumption that K is a sample-independent quantity, this implies that some constraints can be put on the variability of the parameters γ_R and δ_R. In particular, one finds that

$$\gamma_{Sm}^{3/2}\delta_{Sm}^2 \simeq 1.6\gamma_{Ce}^{3/2}\delta_{Ce}^2 \simeq 3\gamma_{La}^{3/2}\delta_{La}^2, \qquad \text{(B10)}$$

as reported in Eq. (10).

*Present address: Leibniz-Institut für Festkörper- und Werkstoffforschung (IFW) Dresden, D-01171 Dresden, Germany; g.prando@ifw-dresden.de

[1] Y. Kamihara, T. Watanabe, M. Hirano, and H. Hosono, J. Am. Chem. Soc. **130**, 3296 (2008).
[2] R. H. Liu, T. Wu, G. Wu, H. Chen, X. F. Wang, Y. L. Xie, J. J. Ying, Y. J. Yan, Q. J. Li, B. C. Shi, W. S. Chu, Z. Y. Wu, and X. H. Chen, Nature (London) **459**, 64 (2009).
[3] L. Boeri, O. V. Dolgov, and A. A. Golubov, Phys. Rev. Lett. **101**, 026403 (2008).
[4] A. Bussmann Holder, A. Simon, H. Keller, and A. R. Bishop, J. Supercond. Nov. Magn. **23**, 365 (2010).
[5] G. A. Ummarino, Phys. Rev. B **83**, 092508 (2011).
[6] F. Hunte, J. Jaroszynski, A. Gurevich, D. C. Larbalestier, R. Jin, A. S. Sefat, M. A. McGuire, B. C. Sales, D. K. Christen, and D. Mandrus, Nature (London) **453**, 903 (2008).
[7] D. Daghero, M. Tortello, R. S. Gonnelli, V. A. Stepanov, N. D. Zhigadlo, and J. Karpinski, Phys. Rev. B **80**, 060502(R) (2009).
[8] S. Weyeneth, M. Bendele, R. Puzniak, F. Murányi, A. Bussmann-Holder, N. D. Zhigadlo, S. Katrych, Z. Bukowski, J. Karpinski, A. Shengelaya, R. Khasanov, and H. Keller, Europhys. Lett. **91**, 47005 (2010).
[9] R. Khasanov, D. V. Evtushinsky, A. Amato, H.-H. Klauss, H. Luetkens, C. Niedermayer, B. Buchner, G. L. Sun, C. T. Lin, J. T. Park, D. S. Inosov, and V. Hinkov, Phys. Rev. Lett. **102**, 187005 (2009).
[10] R. Khasanov, M. Bendele, A. Amato, K. Conder, H. Keller, H.-H. Klauss, H. Luetkens, and E. Pomjakushina, Phys. Rev. Lett. **104**, 087004 (2010).
[11] G. Prando, P. Carretta, R. De Renzi, S. Sanna, A. Palenzona, M. Putti, and M. Tropeano, Phys. Rev. B **83**, 174514 (2011).

[12]D. C. Johnston, Adv. Phys. **59**, 803 (2010).
[13]G. Prando, A. Lascialfari, A. Rigamonti, L. Romano, S. Sanna, M. Putti, and M. Tropeano, Phys. Rev. B **84**, 064507 (2011).
[14]A. Kondrat, J. E. Hamann-Borrero, N. Leps, M. Kosmala, O. Schumann, A. Köhler, J. Werner, G. Behr, M. Braden, R. Klingeler, B. Büchner, and C. Hess, Eur. Phys. J. B **70**, 461 (2009).
[15]X. Zhu, H. Yang, L. Fang, G. Mu, and H.-H. Wen, Supercond. Sci. Technol. **21**, 105001 (2008).
[16]M. Nikolo and R. B. Goldfarb, Phys. Rev. B **39**, 6615 (1989).
[17]F. Gömöry, Supercond. Sci. Technol. **10**, 523 (1997).
[18]A. P. Malozemoff, T. K. Worthington, Y. Yeshurun, F. Holtzberg, and P. H. Kes, Phys. Rev. B **38**, 7203(R) (1988).
[19]M. Tinkham, Phys. Rev. Lett. **61**, 1658 (1988).
[20]C. J. van der Beek and P. H. Kes, Phys. Rev. B **43**, 13032 (1991).
[21]C. J. van der Beek, V. B. Geshkenbein, and V. M. Vinokur, Phys. Rev. B **48**, 3393 (1993).
[22]D. N. Zheng, A. M. Campbell, J. D. Johnson, J. R. Cooper, F. J. Blunt, A. Porch, and P. A. Freeman, Phys. Rev. B **49**, 1417 (1994).
[23]T. T. M. Palstra, B. Batlogg, R. B. van Dover, L. F. Schneemeyer, and J. V. Waszczak, Phys. Rev. B **41**, 6621 (1990).
[24]J. H. P. M. Emmen, V. A. M. Brabers, and W. J. M. de Jonge, Physica C **176**, 137 (1991).
[25]M. Tinkham, Physica B **169**, 66 (1991).
[26]A. Gurevich, Phys. Rev. B **67**, 184515 (2003).
[27]N. R. Werthamer, E. Helfand, and P. C. Hohenberg, Phys. Rev. **147**, 295 (1966).
[28]M. Tinkham, *Introduction to Superconductivity* (McGraw-Hill, New York, 1996).
[29]P. G. de Gennes, *Superconductivity of Metals and Alloys* (Westview Press, Boulder, 1999).
[30]Y. Yeshurun and A. P. Malozemoff, Phys. Rev. Lett. **60**, 2202 (1988).
[31]R. Prozorov, N. Ni, M. A. Tanatar, V. G. Kogan, R. T. Gordon, C. Martin, E. C. Blomberg, P. Prommapan, J. Q. Yan, S. L. Bud'ko, and P. C. Canfield, Phys. Rev. B **78**, 224506 (2008).
[32]A. Rigamonti, F. Borsa, and P. Carretta, Rep. Prog. Phys. **61**, 1367 (1998).
[33]H.-S. Lee, M. Bartkowiak, J. S. Kim, and H.-J. Lee, Phys. Rev. B **82**, 104523 (2010).
[34]X.-L. Wang, S. R. Ghorbani, S.-I. Lee, S. X. Dou, C. T. Lin, T. H. Johansen, K.-H. Muller, Z. X. Cheng, G. Peleckis, M. Shabazi, A. J. Qviller, V. V. Yurchenko, G. L. Sun, and D. L. Sun, Phys. Rev. B **82**, 024525 (2010).
[35]C. J. van der Beek, G. Rizza, M. Konczykowski, P. Fertey, I. Monnet, T. Klein, R. Okazaki, M. Ishikado, H. Kito, A. Iyo, H. Eisaki, S. Shamoto, M. E. Tillman, S. L. Bud'ko, P. C. Canfield, T. Shibauchi, and Y. Matsuda, Phys. Rev. B **81**, 174517 (2010).
[36]G. K. Perkins, L. F. Cohen, A. A. Zhukov, and A. D. Caplin, Phys. Rev. B **51**, 8513 (1995).
[37]I. Pallecchi, C. Fanciulli, M. Tropeano, A. Palenzona, M. Ferretti, A. Malagoli, A. Martinelli, I. Sheikin, M. Putti, and C. Ferdeghini, Phys. Rev. B **79**, 104515 (2009).
[38]J. Jaroszynski, S. C. Riggs, F. Hunte, A. Gurevich, D. C. Larbalestier, G. S. Boebinger, F. F. Balakirev, A. Migliori, Z. A. Ren, W. Lu, J. Yang, X. L. Shen, X. L. Dong, Z. X. Zhao, R. Jin, A. S. Sefat, M. A. McGuire, B. C. Sales, D. K. Christen, and D. Mandrus, Phys. Rev. B **78**, 064511 (2008).
[39]R. Khasanov, H. Luetkens, A. Amato, H.-H. Klauss, Z.-A. Ren, J. Yang, W. Lu, and Z.-X. Zhao, Phys. Rev. B **78**, 092506 (2008).
[40]H. Luetkens, H.-H. Klauss, R. Khasanov, A. Amato, R. Klingeler, I. Hellmann, N. Leps, A. Kondrat, C. Hess, A. Kohler, G. Behr, J. Werner, and B. Buchner, Phys. Rev. Lett. **101**, 097009 (2008), and references therein.
[41]A. Larkin and A. Varlamov, *Theory of Fluctuations in Superconductors* (Oxford Science Publications, Oxford, 2005).
[42]G. Blatter, M. V. Feigel'man, V. B. Geshkenbein, A. I. Larkin, and V. M. Vinokur, Rev. Mod. Phys. **66**, 1125 (1994).